



A simple method of simultaneously endowing paper or fluff pulp with both high softness or appropriate fluffing properties and antimicrobial properties

Yongjian Xu · Yun Shi · Xuyong Chen · Fenfen Liu · Wei Zhao

Received: 6 March 2021 / Accepted: 14 June 2021 / Published online: 21 June 2021
© The Author(s), under exclusive licence to Springer Nature B.V. 2021

Abstract As the living standard improves, disposable sanitary and household paper requires not only softness or easy to fluff in a dry state, but also good antibacterial property. In this study, a series of alkyl quaternary ammonium salts (AQAS), a kinds of antibacterial-debonding agents, were synthesized by using a two-step process. The SN₂ nucleophilic substitution reaction was designed between triethanolamine and sulfoxide chloride, and followed subsequent quaternization by tertiaryamines with different long alkyl chains. The obtained products can be used as an antibacterial and softening/debonding agent for improving the performance of paper or fluff pulp. The results showed that these new compounds can endow antibacterial function and high softness to paper or control appropriate burst strength to fluff pulp. These AQAS products can be not only used in daily disposable sanitary products, but also have potential applications in other products such as

glass spacer paper, advanced household paper, or antibacterial tissue products to prevent microbial contamination.

Keywords Antibacterial activity · Softness · Debonding agent · Fluff pulp · Paper

Introduction

With an improvement in people's living standard, there has been an increasing demand for disposable sanitary products, such as women's sanitary napkins, baby diapers and adult incontinence products (Cordella et al. 2015; Ajmeri and Ajmeri 2016; Widen et al. 2017; Mendoza et al. 2019). Since most disposable sanitary products have close contact with human body, high antibacterial activity during uses is usually desired. However, in most cases, the main material, fluff pulp, used to prepare these disposable sanitary products has no antibacterial activity (Forsgren-Brusk et al. 2017). In addition, a large number of microorganisms exist in the natural environment and they can mass propagate once the conditions are suitable, which can cause bacterial infection and create health problem for people (Asri et al. 2014; Paterson and Harris 2016; Mc Carlie et al. 2020; Wang et al. 2020). Therefore, the development of materials with antibacterial

Supplementary Information The online version contains supplementary material available at <https://doi.org/10.1007/s10570-021-04025-z>.

Y. Xu (✉) · Y. Shi · X. Chen · F. Liu · W. Zhao
College of Bioresources Chemical and Materials
Engineering, Shaanxi Provincial Key Laboratory of
Papermaking Technology and Specialty Paper
Development, National Demonstration Center for
Experimental Light Chemistry Engineering Education,
Shaanxi University of Science and Technology,
Xi'an 710021, Shaanxi Province, China
e-mail: xuyongjian@sust.edu.cn

activity has attracted significant interest in new material research (El-Naggar et al. 2018; Noorian et al. 2020).

In addition, with the increasing demand for household papers, such as toilet paper, napkins, beauty paper and paper towels, there are increasing requirements for quality and performance of these products, especially the softness (Gashti and Adibzadeh 2014). However, in the manufacturing process of household papers, in order to reduce the production costs, a large amount of non-wood and secondary fibers used (Guan et al. 2019; An et al. 2020), which usually makes such products dense and their surface stiff (Illeez et al. 2015; Liu et al. 2020). Although creping is an effective way to increase the softness, it has limited impact. Hence, much attention has been paid to develop novel paper softeners (Tang et al. 2017; Mazzon et al. 2019). In the textile industry, softeners are used widely, but textile softeners are seldom used in papermaking due to some disadvantages, such as the large loading, high cost and poor effectiveness. Therefore, there is a clear need to develop special softening agents for this kind of papers or debonding agents for fluff pulp. In order to make the final tissue products possess high antibacterial activity and at the same time create enough softness or appropriate burst strength, antibacterial agents (Hayashi et al. 2019; Xu et al. 2020) and softening/debonding agent (Igarashi et al. 2016) are usually added together during the papermaking process. However, there are few reports on chemical additives which have both antibacterial and softening/debonding effects. Hence, it is imperative to come up with a concoction as antibacterial-debonding agent to endow paper or fluff pulp with antibacterial and softening/debonding effects.

At present, antibacterial agents have two main types: inorganic and organic agents. Inorganic antibacterial agents such as Au (Lai et al. 2015), Ag (Alahmadi et al. 2018; Caschera et al. 2020; Rabbi et al. 2020; Yousaf et al. 2020), Cu (Jose et al. 2020; Li et al. 2021), TiO₂ (Alizadeh-Sani et al. 2020) and Zn (Zhao et al. 2017; Lallo da Silva et al. 2019; Farooq et al. 2020) and other metal nanoparticles have the advantages of good antibacterial properties, but at the same time there are disadvantages such as easy discoloration, manufacturing difficulties, and complex processes that limit their application in real life. Organic antibacterial agents such as chitosan (Salari et al. 2018; Tu et al. 2019), chlorhexidine (Bashir et al.

2019), triclosan (Alfhili and Lee 2019), polyethyleneimine (Wahid et al. 2019), quaternary ammonium salts (Quinlan et al. 2015; Jiao et al. 2017; Li et al. 2018) have the advantages of fast sterilization speed, strong sterilization ability, convenient processing, and good color stability. The quaternary ammonium salts have been studied by a large number of researchers because of their convenient synthesis and excellent antibacterial ability, and have been greatly developed. Li et al. (Li et al. 2018) achieved functionality by surface modification of cellulose nanocrystals grafted 2-(dimethylamino) ethyl methacrylate (DMAEMA) onto the surface of CNCs to prepare CNCs-g-pdmaema. Subsequently, the tertiary amine group of CNCs-g-PDMAEMA was transferred to the quaternary ammonium group by adding alkyl bromide (C10-C18) with different carbon chain lengths. The results of the study showed that the antimicrobial activity of the prepared antimicrobial materials was related to the alkyl chains of the prepared materials. The best antimicrobial effect was observed for the materials containing C10 alkyl groups in the quaternary ammonium salts.

In a word, compared with other antibacterial agents, organic antibacterial agent with quaternary ammonium group has been widely studied by researchers worldwide because of its advantages of low cost, high antibacterial efficiency, good safety and convenience for applications (Ma et al. 2012; Liu et al. 2015; Jung et al. 2020). Also, the alkyl group on the side chain of QAS has a certain hydrophobicity, which can improve the softness of tissue products (Gao et al. 2019) and may weaken the bonding strength between fibers as debonding agent for fluff pulp.

In this work, a series of multibranch long-chain alkyl quaternary ammonium salt compounds (AQAS), a kind of antibacterial-debonding agents, was synthesized, which played double roles in fluff pulp or paper preparation. Subsequently, the effect of the amount of AQAS on the physical properties of fluff pulp and paper was evaluated and analysed. The softness is changed mainly due to an increase of the length of alkyl chains and the number of long alkyl chains on the side chains in the AQAS molecules. The antibacterial effect is mainly due to an increase of the number of nitrogen positive ions in the AQAS molecules, and the antibacterial properties of the product are measured by the inhibition circle method based on the antibacterial mechanism of nitrogen positive ions. These AQAS

products have potential applications in daily disposable sanitary products and other antibacterial tissue products to prevent microbial contamination. The research results have important application value for developing compound functional chemicals and improving the quality of disposable sanitary products, household paper and industrial paper for special needs.

Materials and methods

Materials

Triethanolamine, ethyl acetate and absolute ethanol were obtained from Tianjin Tianli Chemical Reagent Co., Ltd. Sulfoxide chloride, chloroform, and N,N-dimethylhexadecylamine were obtained from Sino-pharm Chemical Reagent Co., Ltd. N,N-dimethyloctylamine was obtained from Aladdin Reagent Co., Ltd., China. N,N-dimethyltetradecylamine was obtained from TCI Tokyo Chemical Industry Co., Ltd, and all chemicals and reagents were used as received. Bleached softwood and hardwood pulps (in dry lap form) were all provided by Guangxi Fenghuang Co., Ltd., China. In addition, nutrient agar used for antibacterial test was obtained from Beijing Aobox Biotechnology Co., Ltd.

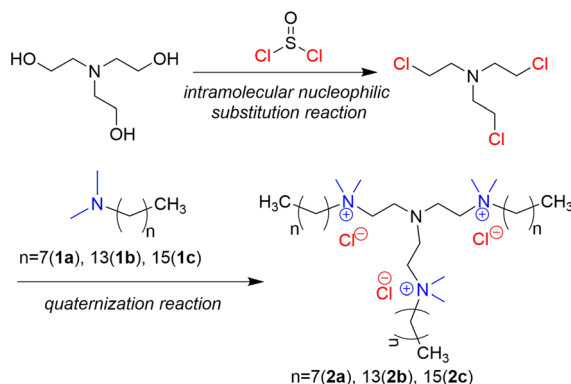
Methods

The synthesis schematic of AQAS

The AQAS with different long alkyl chains was synthesized by using a two-step process. The S_N2 nucleophilic substitution reaction was carried out first via the reaction between triethanolamine and sulfoxide chloride, resulting in tris(2-chloroethy)amine and then long-chain alkyl groups were introduced to the molecule of tris(2-chloroethy)amine by the quaternization reactions with different alkyl tertiaryamines (Scheme 1).

The synthesis of tris(2-chloroethy)amine

Chloroform (0.3 mol) and triethanolamine (0.075 mol) were added into a 250 mL three mouth flask, and then sulfoxide chloride was dropped into the reaction mixture. The above solution was stirred in an ice-water bath. During reaction, there was a slow



Scheme 1 Synthesis schematic of AQAS with different long alkyl chains

release of gas, which was absorbed by the sodium hydroxide solution. After the addition, the reaction temperature was slowly raised to 30 °C and the reactor was kept stirring for 3 h, and then heated up to 60 °C and stirred until no gas was released. Finally, the flask was cooled in ice-water and a large amount of white solid was precipitated, which was then filtered and repeatedly washed with chloroform and ethanol absolute and dried at 50 °C to obtain the intermediate product tris(2-chloroethy)amine hydrochloride white crystals.

The synthesis of AQAS

Tris(2-chloroethy)amine (0.0083 mol) was first added into a 250 mL glass flask. Dilute sodium hydroxide solution was added dropwise into aqueous emulsion to adjust the pH value of the system within a certain range. After heating up to 60 °C, and N,N-dimethyloctylamine (N,N-dimethyl-tetradecylamine and N,N-dimethyl-octadecylamine) (0.0332 mol) were gently dropped into the three flasks to react with the intermediate product. Afterwards, the mixture was stirred at 90 °C for 7 h. Finally, the flask was cooled in ice water bath and a large amount of yellowish solid was separated out, which was then filtered and washed with ethyl acetate and ethanol absolute several times and dried at 50 °C to obtain the product. The products were named as AQAS 2a, AQAS 2b and AQAS 2c.

The preparation of antibacterial paper (or fluff pulp)

AQAS 2a, AQAS 2b and AQAS 2c with concentration of 0.01 g ml^{-1} were added into the pulp suspensions

at 0, 0.25%, 0.5% and 0.75%, respectively. A thorough mixing was provided and paper sheets (or fluff pulp) with the basis weight of 60 g m^{-2} (660 g m^{-2}) were then prepared. The wet sheet was pressed three times under 4 MPa for 2 min, and then the two sides of wet paper was dried for the same time at $105 \text{ }^\circ\text{C}$ in the glazing machine, to ensure the moisture content of the sheet or pad is between 8% ~ 12%. Finally, the dried papers (fluff pulp) were conditioned in sealable bags for 12 h to stabilize the moisture content (Scheme 2).

Characterization

The ^1H nuclear magnetic resonance (^1H NMR) spectrum of AQAS was recorded using an AVII-500 MHz spectrometer (Bruker, Germany) with deuterated chloroform (CDCl_3) as the solvent.

Fourier transform infrared spectroscopy (FTIR) of AQAS was recorded on a spectrometer (VECTOR22, Bruker, Germany) in the range of $400 \sim 4000 \text{ cm}^{-1}$, with an average of 32 scans at the resolution of 4 cm^{-1} . The samples were ground with potassium bromide (KBr) and pressed into transparent pellets..

The burst strength index of fluff pulp was performed on a bursting strength tester (DCP-NPY5600, Changjiang Papermaking Instrument, Sichuan, China) according to GB/T 1539–2007. The fluff-specific volume, absorption rate and absorbility were determined according to GB/T 21,331–2008. The

mechanical performance of each specimen was determined parallelly for three times. The fluff-specific volume (A), absorption rate (B), and absorbility (C) were calculated according to the formula as follow:

$$A = s \cdot h / (10 \cdot x)$$

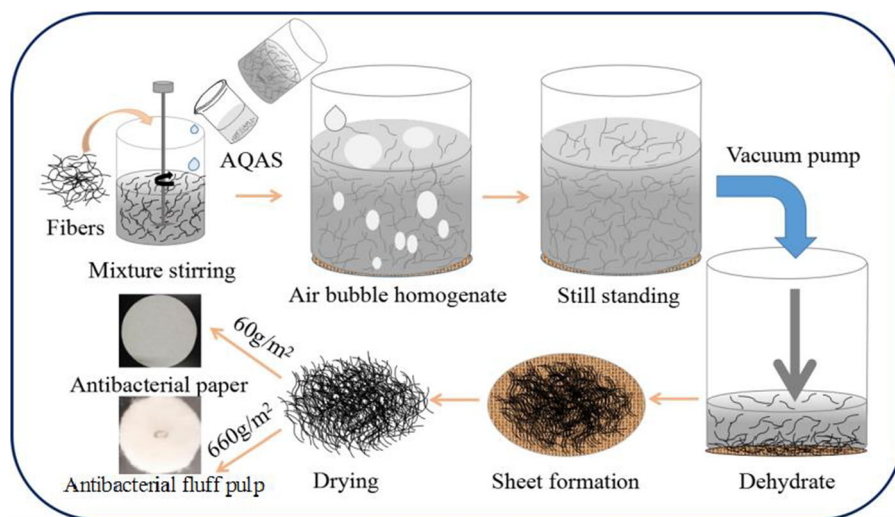
$$B = (y - x) / t$$

$$C = (y - x) / x$$

where s is the area of specimen (19.64 cm^2), h is the initial height of pulp specimens (cm), x is a constant weight (3.00 g) for specimen, y is the weight of specimen with sufficient absorption (g), t is the penetrating time of water from the bottom to top of specimens (s).

The softness of the prepared antibacterial paper was measured on a Tissue Softness Analyzer (Drake Co. Ltd, Shandong, China) according to GB/T 8942 – 2016. Based on the principle, the instrument recorded the maximum vector sum of resistance to bending force of samples and friction between samples and test gap. The smaller of softness value, the more softer of samples.

The surface morphology of antibacterial paper was observed with a scanning electron microscopy (SEM, VEGA 3 S-4800, HITACHI, Tokyo, Japan) at an accelerating voltage of 10 kV. All samples were



Scheme 2 The process of making antibacterial paper and fluff pulp

sputtered with a layer of gold in vacuum for 60 s before analysis.

The antibacterial capability of the prepared antibacterial paper was investigated using the inhibition zone method which is also called the agar disk diffusion method. *E. coil* and *S. aureus* were used in the antibacterial experiment as typical Gram-negative and Gram-positive bacteria, respectively. The medium was prepared as follows: 0.5 g beef extract, 0.5 g sodium chloride, 1.0 g peptone and 1.5 g agar were added into 100 mL distilled water and autoclaved at 121 °C for 15 min. Then 20 mL medium was poured into the sterilized petri dish. After the medium was solidified, 50 mL bacterial suspensions were uniformly smeared over the dish. Then, the cellulosic specimens were cut into circles with a diameter of 12 mm and then were gently placed on Petri dishes. After being incubated for 24 h at 37 °C under 50% relative humidity, the diameter (mm) of the inhibition zone was calculated using the following formula:

$$H = (D - d)/2$$

where H is the bacteriostatic belt width, D is the average outside diameter of inhibition zone, and d is the diameter of the specimens or the control ones.

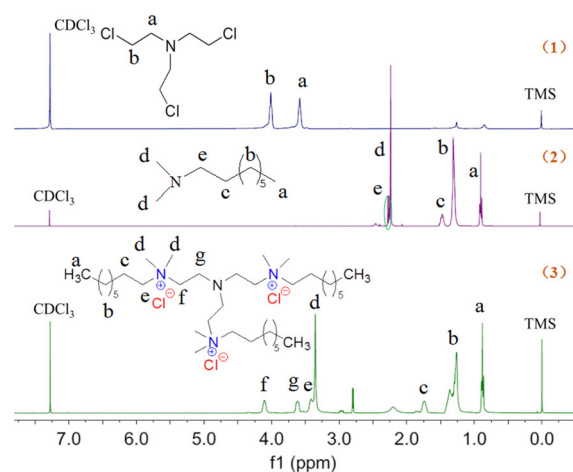


Fig. 1 ^1H NMR spectra of **1** tris(2-chloroethyl)amine, **2** N,N-dimethyloctylamine and **3** AQAS 2a

Results and discussion

The ^1H NMR and FT-IR spectra analysis of AQAS 2a

The ^1H NMR spectra (500 MHz, CDCl_3 , 25 °C) of AQAS 2a is shown in Fig. 1. The peaks at 0.88, 1.26 and 1.74 ppm originate from the AQAS 2a are attributed to the terminal methyl of $-\text{CH}_2-\text{CH}_3$, side chain methylene group ($(-\text{CH}_2)_5$) of AQAS 2a and methylene of $\text{N}^+-\text{CH}_2-\text{CH}_2-$, respectively. The peak at 3.35 ppm belongs to methyl of N^+-CH_3 , the peak at 3.42 ppm is attributed to the methylene ($\text{N}^+-\text{CH}_2-\text{CH}_2-\text{CH}_2-$) of AQAS 2a and the methylene peak of $\text{N}-\text{CH}_2$ was observed at 3.62 ppm. In addition, the peak at 4.11 ppm assigned to methylene of $\text{N}-\text{CH}_2-\text{CH}_2$ (Kang et al. 2016), indicates that the target product has been successfully synthesized (Fig. 1). However, the methyl peak (2.79 ppm) in $-\text{CH}_2-\text{CH}_3$, methylene peak (2.94 ppm) in $\text{N}^+-\text{CH}_2-\text{CH}_2-$, and the peak of N^+-H at around 2.21 ppm are also weakly observed in Fig. 1, which indicates the presence of by-products (tertiary ammonium hydrochloride) in terminal product.

The AQAS 2a was further characterized by FT-IR spectra (Fig. 2). The strong absorption peak at 1470 cm^{-1} belongs to methyl bending vibration peak in $\text{N}^+-\text{(CH}_3)_2$, and the symmetric bending vibration absorption peak of methyl in $-\text{CH}_2-\text{CH}_3$ could be observed at 1379 cm^{-1} , which is a characteristic

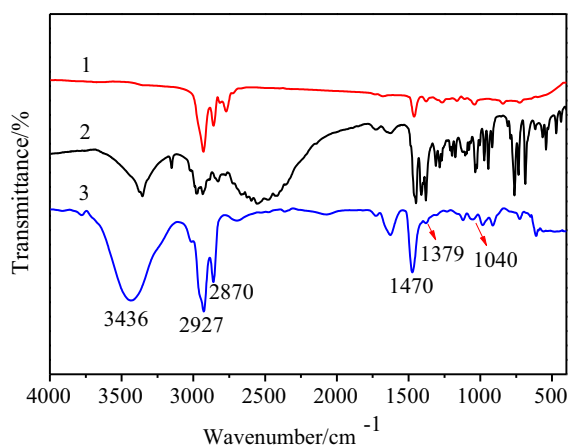


Fig. 2 FT-IR spectra. **1**. N,N-dimethyl-octylamine, **2**. tris(2-chloroethyl)amine and **3**. AQAS 2a

absorption peak of moderate intensity. The weak absorption peak near 1040 cm^{-1} is the characteristic absorption frequency of quaternary ammonium salt, which confirms the formation of AQAS 2a. Compared with Line 2 in Fig. 2, the characteristic absorption peaks of methyl and quaternary ammonium salt group appear for the first time. Besides, there still exist the methylene asymmetric and symmetric stretching vibration absorption peaks at 2927 cm^{-1} and

2870 cm^{-1} region in $\text{NR}_2\text{-CH}_2\text{-R}$. In addition, the strong absorption peak at 760 cm^{-1} is weakened, which indicates the weakened C–Cl stretching vibration peak in $\text{-CH}_2\text{-Cl}$. This may be attributed to the presence of by-products that incomplete quaternary ammonium salt in the product. We successfully synthesized AQAS 2b and AQAS 2c by using a similar method to AQAS 2a. For detailed characterization and spectra please refer to the supporting information (Fig. S1, Fig. S2, Fig. S3, Fig. S4).

The properties of the fluff pulp and fluff fiber

Apparent density and burst strength index of the fluff pulp

As shown in Fig. 3a, b, the apparent density and burst strength index of the fluff pulp decrease with increasing the addition of AQAS, and the decrease is more significant with the increase of the addition. The decreasing trend of the apparent density and burst strength index becomes flat after the amount of AQAS is more than 0.75%. The apparent density of fluff pulp is defined as the ratio of the basis weight of fluff pulp to its thickness. The burst strength index of fluff pulp was measured according to GB/T 1539–2007. It is the ratio of the average burst strength of fluff pulp to its basis weight. It can speculate there is no simple liner relationship between them because of the change in the thickness. From these experiment results, it is deduced that AQAS treatment can shield hydroxyl groups on the surface of fibers, resulting the bonding force weaker between fibers and the volume of fluff pulp increase. Then the apparent density and burst strength index of the fluff pulp decrease with increasing the addition of AQAS. The effect of long alkyl chain is clearer.

Water absorptibility and water absorption rate of the fluff fibers

As the amount of AQAS increased, the water absorptibility and water absorption rate of fluff pulp show a decreasing trend (Fig. 3c, d). When the amount of AQAS is up to 0.5%, the decreasing trend is gradually leveled off. The alkyl chain in AQAS plays the role of shielding hydroxyl group, and with the increase of AQAS, the shielding effect becomes more clear. The longer the alkyl chain, the greater the shielding effect of the hydroxyl group. More alkyl groups with hydrophobic effect are attached to the surface of the fluff pulp fibers, resulting in lower absorptibility of the fibers and consequently lower water absorption rate of the fluff pulp.

Fluff-specific volume of the fluff pulp

As shown in Fig. 3e, with increasing the addition of AQAS, the fluff-specific volume tends to rise first and then fall. The three hydrophobic alkyl chains in AQAS on the fiber surface hinder the combination between fibers, making the gap between fibers increase and become fluffy, so that the fluff-specific volume of the fluff pulp is on the rise, and when the amount of AQAS is high, the three long alkyl chains in AQAS are easy to cross and entangle with each other, so that when the pulp is dry dissociated, the fiber network is uneven and appears to be knotted and fall off in pieces. It affects the fluff-specific volume of antibacterial pulp fiber.

The surface morphology of fluff fibers

Surface morphology of antibacterial fluff pulp fibers with AQAS 2c was examined using SEM as shown in Fig. 4, we can see that the surface of fibers in the blank sample is very rough, and some microfibrils are broken away from the surface. This would have an adverse impact on the softness of fluff pulp. However, the SEM images of fluff pulp fibers treated by AQAS 2c show that the fiber surface is smoother with the increase of the loading of AQAS 2c. Therefore, adding proper amounts of AQAS 2c to pulp fiber is an effective way of improving the softness of antibacterial paper.

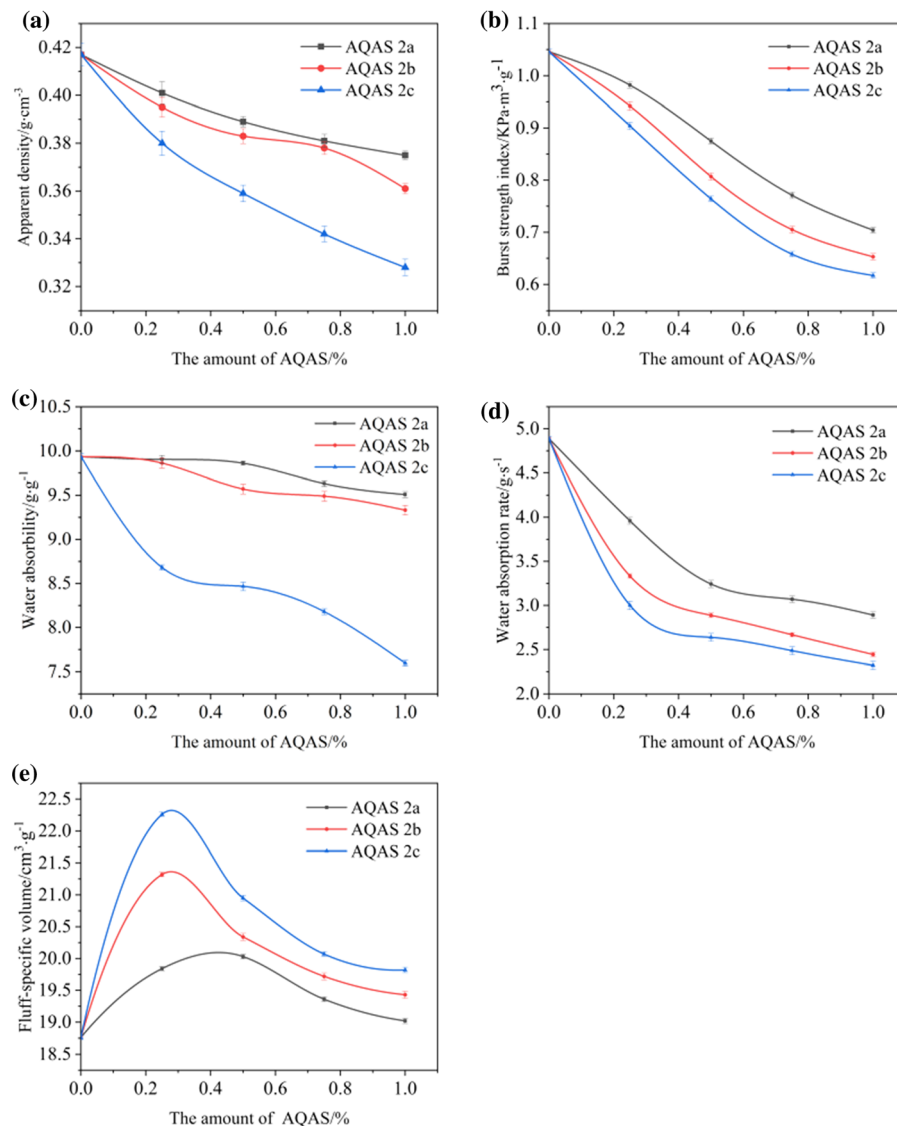


Fig. 3 The properties with the loading amounts of AQAS for fluff pulp **a** apparent density, **b** burst strength index, and for fluff fiber **c** water absorptivity, **d** water absorption rate, and **e** fluff-specific volume

The air permeability and softness of antibacterial paper

In order to explore the effect of AQAS 2a, AQAS 2b and AQAS 2c on the air permeability and softness of antibacterial paper, the different amounts of AQAS were added into pulp suspension to make paper with the basis weight of 60 g m^{-2} (Scheme 2), and the testing results are shown in Fig. 5.

The air permeability of paper gradually increases with the amount of AQAS increases, the shielding

effect of alkyl chains on fiber hydroxyl groups also increases, and the bonding force between pulp fibers decreases (Fig. 5a). The reason is that the hydrogen bonds between fibers can not form when the AQAS was used. On the other hand, the three hydrophobic alkyl chains in AQAS on the fiber surface hinder the combination between fibers. And the long alkyl-chains in AQAS may tend to cross and tangle with each other, which makes the paper become bulky and the air permeability increase. When the amount of AQAS is below 0.25%, that AQAS

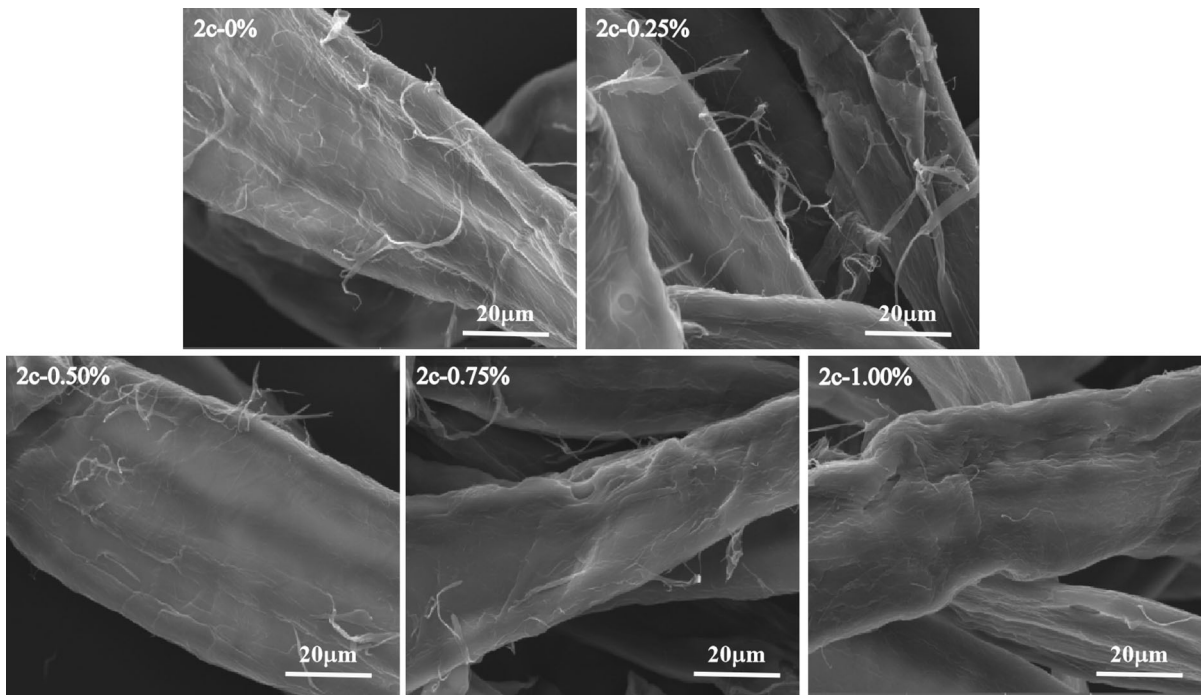


Fig. 4 The surface morphology of fibers with different loading amounts of AQAS 2c

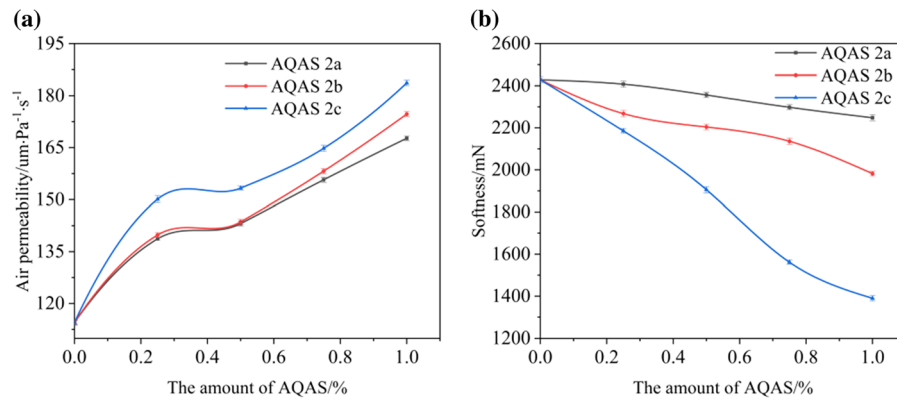


Fig. 5 The properties of paper with different loading amounts of AQAS. **a** air permeability, **b** softness

quickly shields free hydroxyl groups on the surface of fibers. When the amount of AQAS is between 0.25%–0.5%, the shielding effect on the hydroxyl group may have a lag effect because the free hydroxyl groups are derived from fracturing hydrogen bond fracturing, and then the change for air permeability gradually flattened. When the amount of AQAS is more than 0.5%, AQAS fills the fiber void, a physical phenomenon, thus

the gap between fibers increases and the paper becomes bulky. There may be a replacement between AQAS and water in the form of hydrogen bonds with the hydroxyl groups of cellulose.

As shown in Fig. 5b, the softness of control sample is 2428.5 mN. The softness of paper decreased with increasing the amount of AQAS, indicating that the softness is constantly improved. The result

supports the conclusion that AQAS 2a, AQAS 2b and AQAS 2c also have softening effect. Moreover, it is found that the softness of all samples decrease slowly with the AQAS loading up to 0.25wt%. When their loading is more than 0.25wt%, the softness of paper adding AQAS 2a or AQAS 2b also drops slowly, but the decreasing trend is clear for adding AQAS 2c. This indicates for AQAS 2c can endow paper the best softening effect. It may be attributed to the alkyl groups with hydrophobicity of AQAS 2c which are more than that of AQAS 2a and AQAS 2b. The alkyl groups can form hydrophobic external reverse adsorption on the surface of fibers, and reduce the dynamic and static friction factors of paper fiber. Therefore, the AQAS 2c can be used as a softener with antibacterial activity for tissue papermaking. According to the former research by our team, when the amount of commercial debonding agent were 0.25%, 0.5%, 0.75%, 1.0%, the softness were 2421mN, 1872mN, 1473mN and 1339mN, respectively. When the amount of AQAS was 0.25%, the softness were from top to bottom AQAS 2c, AQAS 2b, AQAS 2a, commercial debonding agent. When the amount was more than 0.5%, the softness of commercial debonding agent was near by AQAS 2c, the softness of AQAS 2b and AQAS 2a were general.

The antibacterial activity of fluff pulp and paper

The antibacterial activity testing results are shown in Fig. 6. It was found that no inhibition zone appeared around the blank sample, indicating the poor

antibacterial activity for original fiber. However, the inhibition zone appeared for other samples of paper made with AQAS 2a (AQAS 2b, AQAS 2c), and the inhibition zone increased with the increase of the loading amount of AQAS, which all confirmed the addition of 2a (2b, 2c) imparted fluff pulp with antibacterial activity. AQAS 2a, AQAS 2b and AQAS 2c are excellent antibacterial agents against *S. aureus* and *E. coli*. Compared with the cellulose-based Schiff base-Cu (II) antibacterial complex (5.5 mm) (Xu et al., 2020), this antibacterial paper of this study shows larger inhibition zone width.

The comparison of antibacterial activity of different AQAS is shown in Fig. 7. As can be seen on the two plates, the diameter of inhibition zone around the samples decreased significantly with the increase of alkyl group on the side chain of AQAS, which means the antibacterial activity of AQAS 2a is the strongest against either *S. aureus* or *E. coli*, the second is AQAS 2b, and the antibacterial activity of AQAS 2c is the weakest. Furthermore, compared with *E. coli*, the antibacterial activity of fluff pulp with different AQAS against *S. aureus* is better, which is consistent with the above conclusion in Fig. 3.

The antibacterial and softening mechanism of AQAS

As shown in Scheme 3, when a certain loading of AQAS is added to the pulp fiber, the AQAS can be attached to the fiber surface by electrostatic adsorption to form something like water film. Then it hinders the

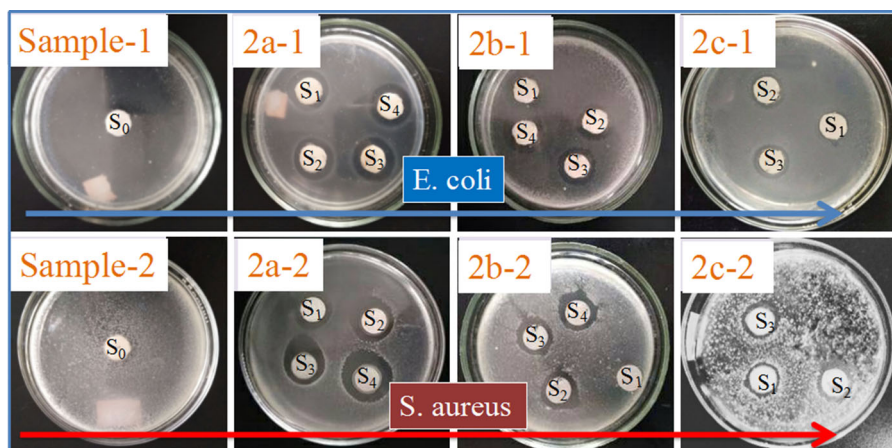


Fig. 6 Antibacterial activity of fluff pulp with different loading amount of AQAS 2a, AQAS 2b and AQAS 2c. S₀, S₁, S₂, S₃ and S₄ stand for the amount of 0, 0.25%, 0.5%, 0.75% and 1.0%, respectively

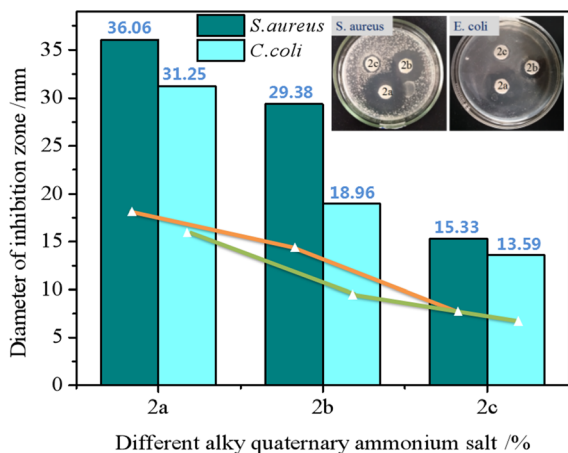


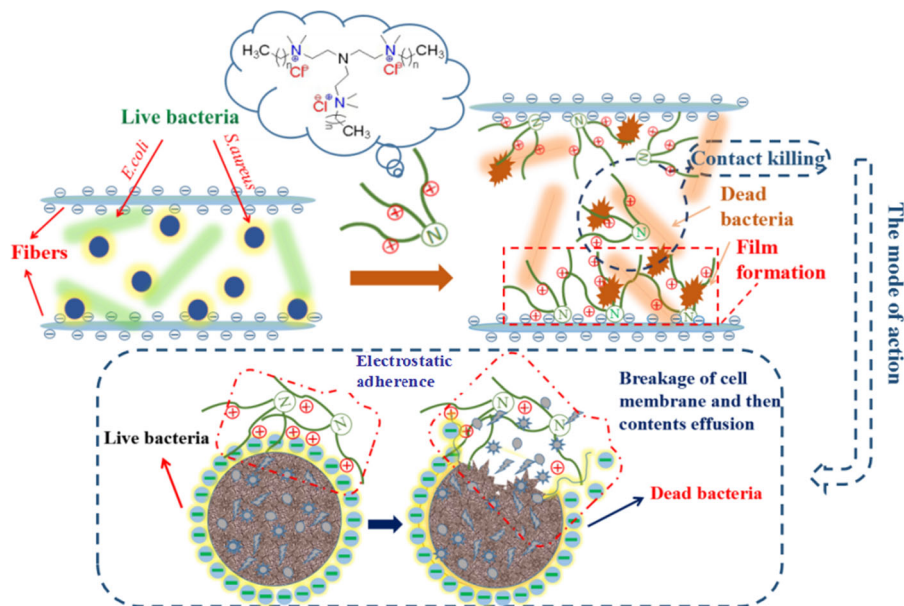
Fig. 7 Antibacterial activity of fluff pulp with different AQAS

bacteria from getting closer to achieve certain antibacterial effect. Besides, the AQAS contacts with the surface of bacteria, and the structure of bacteria cell membrane is destroyed, so that the bacteria die (Jung et al. 2019), to achieve the purpose of sterilization. The nitrogen positive ions in the AQAS is the active species in the bactericidal mechanism. The bactericidal mechanism for *S. aureus* is similar with *E. coli*. However, the softening effect can be attributed to:

(1) the quaternary nitrogen positive ions combine with free hydroxyl groups on the surface of fibers, reduce the formation of hydrogen bonds, weaken the bond between fibers, decrease the static friction coefficient between fibers, and then the surface of the fibers become smoother, (2) long alkyl chains have a certain hydrophobicity, which reduces the formation of hydrogen bonds between fibers and makes the structure of fibers looser. Therefore, both of them can make the antibacterial products have certain softening effect, and control the burst strength of fluff pulp suitable for dry disintegration.

Conclusions

The antibacterial effect is created mainly by increasing the number of nitrogen positive ions in the AQAS molecule, based on the antibacterial mechanism of nitrogen positive ions to achieve the purpose of product antibacterial. The softness is increased mainly by increasing the length of alkyl chains and the number of long alkyl chains on the side chains of AQAS molecules, relying on the hydrophobicity of alkyl chains, reducing the hydrogen bonding, and using electrostatic adsorption to attach to the fiber surface, reducing the static friction coefficient



Scheme 3 The antibacterial and softening schematic of AQAS

between fibers, so that the product has a certain degree of softness.

A series of AQAS products were successfully synthesized and evaluated as antibacterial and softening agents in paper making and debonding agents in fluff pulp. The obtained fluff pulp and paper with these AQAS products showed excellent antibacterial activity against *S. aureus* and *E. coli*. At the same time, the softness for the antibacterial tissue and the burst strength for antibacterial fluff pulp has been improved. These AQAS products can be used in daily disposable sanitary products, but also have potential applications in other products such as Liquid Crystal Display (LCD) glass spacer paper, premium household paper, or antibacterial tissue products to prevent microbial contamination.

Acknowledgments The authors are grateful for the support of the Open Fund of the State Key Laboratory of Pulp and Paper Engineering, South China University of Technology (201730); National Demonstration Center for Experimental Light Chemistry Engineering Education, Shaanxi University of Science and Technology; Key Scientific Research Group of Shaanxi Province (2017KCT-02) and Shaanxi University of Science and Technology Academic Leader Training Program (2013XSD25).

Data availability Data and materials are available.

Declarations

Conflict of interest The authors declare that they do not have any conflict of interest.

Human and animal participants This manuscript does not involve animal studies or human participants in the study.

References

- Ajmeri JR, Ajmeri CJ (2016). Developments in the use of nonwovens for disposable hygiene products. <https://doi.org/10.1016/b978-0-08-100575-0.00018-8>
- Alahmadi NS, Betts JW, Heinze T, Kelly SM, Koschella A, Wadhawan JD (2018) Synthesis and antimicrobial effects of highly dispersed, cellulose-stabilized silver/cellulose nanocomposites. *RSC Adv* 8(7):3646–3656. <https://doi.org/10.1039/c7ra12280b>
- Alfhili MA, Lee M-H (2019) Triclosan: an update on biochemical and molecular mechanisms. *Oxid Med Cell Longev* 2019:1–28. <https://doi.org/10.1155/2019/1607304>
- Alizadeh-Sani M, Mohammadian E, McClements DJ (2020) Eco-friendly active packaging consisting of nanostructured biopolymer matrix reinforced with TiO₂ and essential oil: application for preservation of refrigerated meat. *Food Chem* 322:126782. <https://doi.org/10.1016/j.foodchem.2020.126782>
- An X, Liu J, Liu L, Zhang H, Nie S, Cao H, Xu Q, Liu H (2020) Improving the flexibility of bamboo mechanical pulp fibers for production of high soft tissue handsheets. *Ind Crops Prod*. <https://doi.org/10.1016/j.indcrop.2020.112410>
- Asri LATW, Crismaru M, Roest S, Chen Y, Ivashenko O, Rudolf P, Tiller JC, van der Mei HC, Loontjens TJA, Busscher HJ (2014) A shape- adaptive, antibacterial-coating of immobilized quaternary- ammonium compounds tethered on hyperbranched polyurea and its mechanism of action. *Adv Func Mater* 24(3):346–355. <https://doi.org/10.1002/adfm.201301686>
- Bashir MH, Hollingsworth A, Schwab D, Prinsen KS, Paulson JE, Morse DJ, Bernatchez SF (2019) Ex vivo and in vivo evaluation of residual chlorhexidine gluconate on skin following repetitive exposure to saline and wiping with 2% chlorhexidine gluconate/70% isopropyl alcohol pre-operative skin preparations. *J Hosp Infect* 102(3):256–261. <https://doi.org/10.1016/j.jhin.2018.10.004>
- Caschera D, Toro RG, Federici F, Montanari R, de Caro T, Al-Shemy MT, Adel AM (2020) Green approach for the fabrication of silver-oxidized cellulose nanocomposite with antibacterial properties. *Cellulose* 27(14):8059–8073. <https://doi.org/10.1007/s10570-020-03364-7>
- Cordella M, Bauer I, Lehmann A, Schulz M, Wolf O (2015) Evolution of disposable baby diapers in Europe: life cycle assessment of environmental impacts and identification of key areas of improvement. *J Clean Prod* 95:322–331. <https://doi.org/10.1016/j.jclepro.2015.02.040>
- El-Naggar ME, Shaarawy S, Hebeish AA (2018) Multifunctional properties of cotton fabrics coated with in situ synthesis of zinc oxide nanoparticles capped with date seed extract. *Carbohydr Polym* 181:307–316. <https://doi.org/10.1016/j.carbpol.2017.10.074>
- Farooq A, Patoary MK, Zhang M, Mussana H, Li M, Naem MA, Mushtaq M, Farooq A, Liu L (2020) Cellulose from sources to nanocellulose and an overview of synthesis and properties of nanocellulose/zinc oxide nanocomposite materials. *Int J Biol Macromol* 154:1050–1073. <https://doi.org/10.1016/j.ijbiomac.2020.03.163>
- Forsgren-Brusk U, Yhlen B, Blomqvist M, Larsson P (2017) Method for bacterial growth and ammonia production and effect of inhibitory substances in disposable absorbent hygiene products. *J Wound Ostomy Cont Nurs* 44(1):78–83. <https://doi.org/10.1097/won.0000000000000275>
- Gao D, Li Y, Lyu B, Jin D, Ma J (2019) Silicone quaternary ammonium salt based nanocomposite: a long-acting antibacterial cotton fabric finishing agent with good softness and air permeability. *Cellulose* 27(2):1055–1069. <https://doi.org/10.1007/s10570-019-02832-z>
- Gashti MP, Adibzadeh H (2014) Ultrasound for efficient emulsification and uniform coating of an anionic lubricant on cotton. *Fibers Polym* 15(1):65–70. <https://doi.org/10.1007/s12221-014-0065-7>
- Guan M, An X, Liu H (2019) Cellulose nanofiber (CNF) as a versatile filler for the preparation of bamboo pulp based tissue paper handsheets. *Cellulose* 26(4):2613–2624. <https://doi.org/10.1007/s10570-018-2212-6>

- Hayashi K, Nozaki K, Tan Z, Fujita K, Nemoto R, Yamashita K, Miura H, Itaka K, Ohara S (2019) Enhanced antibacterial property of facet-engineered TiO₂ nanosheet in presence and absence of ultraviolet irradiation. *Materials*. <https://doi.org/10.3390/ma13010078>
- Igarashi T, Nakamura K, Hoshi M, Hara T, Kojima H, Itou M, Ikeda R, Okamoto Y (2016) Elucidation of softening mechanism in rinse-cycle fabric softeners. part 2: uneven adsorption-the key phenomenon to the effect of fabric softeners. *J Surfactants Deterg* 19:759–773. <https://doi.org/10.1007/s11743-016-1815-x>
- İllez AA, Dalbaşı ES, Kayseri GÖ (2015) Improving of sewability properties of various knitted fabrics with the softeners. *Procedia Soc Behav Sci* 195:2786–2795. <https://doi.org/10.1016/j.sbspro.2015.06.394>
- Jiao Y, Niu L-n, Ma S, Li J, Tay FR, Chen J-h (2017) Quaternary ammonium-based biomedical materials: state-of-the-art, toxicological aspects and antimicrobial resistance. *Prog Polym Sci* 71:53–90. <https://doi.org/10.1016/j.propolymsci.2017.03.001>
- Jose M, Szymańska K, Szymański K, Moszyński D, Mozia S (2020) Effect of copper salts on the characteristics and antibacterial activity of Cu-modified titanate nanotubes. *J Environ Chem Eng* 8(6):104550. <https://doi.org/10.1016/j.jece.2020.104550>
- Jung J, Wen J, Sun Y (2019) Amphiphilic quaternary ammonium chitosans self-assemble onto bacterial and fungal biofilms and kill adherent microorganisms. *Colloids Surf B Biointerfaces* 174:1–8. <https://doi.org/10.1016/j.colsurfb.2018.10.078>
- Jung J, Bae Y, Kwan Cho Y, Ren X, Sun Y (2020) Structural insights into conformation of amphiphilic quaternary ammonium chitosans to control fungicidal and anti-biofilm functions. *Carbohydr Polym* 228:115391. <https://doi.org/10.1016/j.carbpol.2019.115391>
- Kang CK, Kim SS, Kim S, Lee J, Lee JH, Roh C, Lee J (2016) Antibacterial cotton fibers treated with silver nanoparticles and quaternary ammonium salts. *Carbohydr Polym* 151:1012–1018. <https://doi.org/10.1016/j.carbpol.2016.06.043>
- K-pM T, Kan C-w, Fan J-t, Tso S-l (2017) Effect of softener and wetting agent on improving the flammability, comfort, and mechanical properties of flame-retardant finished cotton fabric. *Cellulose* 24(6):2619–2634. <https://doi.org/10.1007/s10570-017-1268-z>
- Lai H-Z, Chen W-Y, Wu C-Y, Chen Y-C (2015) Potent Antibacterial Nanoparticles for Pathogenic Bacteria. *ACS Appl Mater Interfaces* 7(3):2046–2054. <https://doi.org/10.1021/am507919m>
- Lallo da Silva B, Caetano BL, Chiari-Andréo BG, Pietro RCLR, Chiavacci LA (2019) Increased antibacterial activity of ZnO nanoparticles: influence of size and surface modification. *Colloids Surf, B* 177:440–447. <https://doi.org/10.1016/j.colsurfb.2019.02.013>
- Li M, Liu X, Liu N, Guo Z, Singh PK, Fu S (2018) Effect of surface wettability on the antibacterial activity of nanocellulose-based material with quaternary ammonium groups. *Colloids Surf, A* 554:122–128. <https://doi.org/10.1016/j.colsurfa.2018.06.031>
- Li M, Nan L, Liang C, Sun Z, Yang L, Yang K (2021) Antibacterial behavior and related mechanisms of martensitic Cu-bearing stainless steel evaluated by a mixed infection model of *Escherichia coli* and *Staphylococcus aureus* in vitro. *J Mater Sci Technol* 62:139–147. <https://doi.org/10.1016/j.jmst.2020.05.030>
- Liu WS, Wang CH, Sun JF, Hou GG, Wang YP, Qu RJ (2015) Synthesis, characterization and antibacterial properties of dihydroxy quaternary ammonium salts with long chain alkyl bromides. *Chem Biol Drug Des* 85(1):91–97. <https://doi.org/10.1111/cbdd.12427>
- Liu D, Yang X, Liu P, Mao T, Shang X, Wang L (2020) Synthesis and characterization of gemini ester surfactant and its application in efficient fabric softening. *J Mol Liq*. <https://doi.org/10.1016/j.molliq.2019.112236>
- Ma S, Izutani N, Imazato S, Chen J-h, Kiba W, Yoshikawa R, Takeda K, Kitagawa H, Ebisu S (2012) Assessment of bactericidal effects of quaternary ammonium-based antibacterial monomers in combination with colloidal platinum nanoparticles. *Dent Mater J* 31(1):150–156. <https://doi.org/10.4012/dmj.2011-180>
- Mazzon G, Zahid M, Heredia-Guerrero JA, Balliana E, Zendri E, Athanassiou A, Bayer IS (2019) Hydrophobic treatment of woven cotton fabrics with polyurethane modified aminosilicone emulsions. *Appl Surf Sci* 490:331–342. <https://doi.org/10.1016/j.apsusc.2019.06.069>
- Mc Carlie S, Boucher CE, Bragg RR (2020) Molecular basis of bacterial disinfectant resistance. *Drug Resist Updat* 48:100672. <https://doi.org/10.1016/j.drugp.2019.100672>
- Mendoza JMF, D'Aponte F, Gualtieri D, Azapagic A (2019) Disposable baby diapers: life cycle costs, eco-efficiency and circular economy. *J Clean Prod* 211:455–467. <https://doi.org/10.1016/j.jclepro.2018.11.146>
- Noorian SA, Hemmatinejad N, Navarro JAR (2020) Ligand modified cellulose fabrics as support of zinc oxide nanoparticles for UV protection and antimicrobial activities. *Int J Biol Macromol* 154:1215–1226. <https://doi.org/10.1016/j.ijbiomac.2019.10.276>
- Paterson DL, Harris PNA (2016) Colistin resistance: a major breach in our last line of defence. *Lancet Infect Dis* 16(2):132–133. [https://doi.org/10.1016/s1473-3099\(15\)00463-6](https://doi.org/10.1016/s1473-3099(15)00463-6)
- Quinlan PJ, Tanvir A, Tam KC (2015) Application of the central composite design to study the flocculation of an anionic azo dye using quaternized cellulose nanofibrils. *Carbohydr Polym* 133:80–89. <https://doi.org/10.1016/j.carbpol.2015.06.095>
- Rabbi MA, Rahman MM, Minami H, Habib MR, Ahmad H (2020) Ag impregnated sub-micrometer crystalline jute cellulose particles: catalytic and antibacterial properties. *Carbohydr Polym* 233:115842. <https://doi.org/10.1016/j.carbpol.2020.115842>
- Salari M, Sowti Khiabani M, Rezaei Mokarram R, Ghanbarzadeh B, Samadi Kafil H (2018) Development and evaluation of chitosan based active nanocomposite films containing bacterial cellulose nanocrystals and silver nanoparticles. *Food Hydrocoll* 84:414–423. <https://doi.org/10.1016/j.foodhyd.2018.05.037>
- Tu C, Zhang R-d, Yan C, Guo Y, Cui L (2019) A pH indicating carboxymethyl cellulose/chitosan sponge for visual monitoring of wound healing. *Cellulose* 26(7):4541–4552. <https://doi.org/10.1007/s10570-019-02378-0>

- Wahid F, Bai H, Wang F-P, Xie Y-Y, Zhang Y-W, Chu L-Q, Jia S-R, Zhong C (2019) Facile synthesis of bacterial cellulose and polyethyleneimine based hybrid hydrogels for antibacterial applications. *Cellulose* 27(1):369–383. <https://doi.org/10.1007/s10570-019-02806-1>
- Wang Y, Yang Y, Shi Y, Song H, Yu C (2020) Antibiotic-free antibacterial strategies enabled by nanomaterials: progress and perspectives. *Adv Mater* 32(18):e1904106. <https://doi.org/10.1002/adma.201904106>
- Widen H, Alenljung S, Forsgren-Brusk U, Hall G (2017) Sensory characterization of odors in used disposable absorbent incontinence products. *J Wound Ostomy Continence Nurs* 44(3):277–282. <https://doi.org/10.1097/WON.0000000000000326>
- Xu Y, Shi Y, Lei F, Dai L (2020) A novel and green cellulose-based schiff base-Cu (II) complex and its excellent antibacterial activity. *Carbohydr Polym* 230:115671. <https://doi.org/10.1016/j.carbpol.2019.115671>
- Yousaf H, Mehmood A, Ahmad KS, Raffi M (2020) Green synthesis of silver nanoparticles and their applications as an alternative antibacterial and antioxidant agents. *Mater Sci Eng C* 112:110901. <https://doi.org/10.1016/j.msec.2020.110901>
- Zhao S-W, Zheng M, Zou X-H, Guo Y, Pan Q-J (2017) Self-assembly of hierarchically structured cellulose@ZnO composite in solid-liquid homogeneous phase: synthesis, dft calculations, and enhanced antibacterial activities. *ACS Sustain Chem Eng* 5(8):6585–6596. <https://doi.org/10.1021/acssuschemeng.7b00842>

Publisher's Note Springer Nature remains neutral with regard to jurisdictional claims in published maps and institutional affiliations.